ROBUST FRAMEWORK FOR DIGITAL IMAGE DENOISING AND DEBLURRING

KENNY TOH KAL VIN

UNIVERSITI SAINS MALAYSIA

2012

ROBUST FRAMEWORK FOR DIGITAL IMAGE DENOISING AND DEBLURRING

by

KENNY TOH KAL VIN

Thesis submitted in fulfilment of the requirements
for the degree of
Doctor of Philosophy

June 2012

ACKNOWLEDGEMENTS

This is the part of the thesis that is the most fun to write. It is also the most difficult because few lines of acknowledgment do not fully express my appreciation and gratitude for those who have guided and supported me through thick and thin. I must say it was their sincere assistance and support that helped me to reach this milestone.

First and foremost, I wish to express my gratitude to Assoc. Prof. Dr. Nor Ashidi Mat Isa for his support and guidance, without which I would have not gotten this far. I consider myself lucky in having the privilege and honor to conduct research under his watchful eyes. His constructive criticism and incisive feedback have helped to bring this research to a satisfactory completion. I am also grateful for his empathy, friendship, and great sense of humor. I especially want to thank him for giving me sufficient intellectual freedom to pursue my own ideas and directions, while making sure I stayed on track.

Many thanks to Prof. Mohd Zaid Abdullah who has always been supportive throughout the tumultuous time, and not to forget his useful comments that have helped to refine this thesis. Special thanks to Prof. Lim Chee Peng for his early advice in research ethics. I am grateful to my thesis examiners, Prof. Surendra Ranganath and Dr. Khoo Bee Ee, for their invaluable advice in improving this thesis. I also take this opportunity to thank Pn. Sarina Razak, En. Rahmat Ariffin, and En. Sazali Ramli for their readiness to look into any administrative issues, and never fail in solving them. Finally, I wish to acknowledge the Universiti Sains Malaysia for funding my studies through the Fellowship Scheme and Postgraduate Research Grant Scheme (PRGS),[1] which I have held for the past three years.

The Imaging and Intelligent Systems Research Team (ISRT) Lab has played a very important role in my years as a graduate student, and I thank my colleagues for making them

[1]The research in this thesis has also been supported in part by the PRGS grant USM-RU-PRGS 1001/PELECT/8032052, titled “Noise Reduction for Digital Image.”

enjoyable and fun. I spent much time talking to former colleagues, Ooi Chen Hee and Tan Khang Siang, about half-baked ideas, and the robust framework came from bouncing ideas back-and-forth with them. I would also like to thank Naim Jain, Chan Keam Seng, Helmi Suid, Oong Tat Hee, Siti Noraini, Ting Shyue Siong, Khairunnisa Hasikin, Lee Wee Chuen, Intan Aidha, and Lim Wei Hong, who have always been there to talk about technical problems and, generally, provide me comical relief.

Above all, this thesis is dedicated to my family. I thank my parents, brothers, and the rest of my family, for their unfailing care, love, sacrifice, and support. I am grateful to my parents for always reminding me that I could achieve whatever I wanted. As my journey being a student draws to an end, I wish all parents would remind their schooling children the same, and to provide them with the unconditional love and support that I have been lucky enough to receive.

Finally, Tan Lay Yong deserves more thanks than can be put into words. She is the one behind the scenes, whom I shared all the ecstatic moments and despairs that accompany this thesis. I sincerely thank her for her love, understanding, encouragement, support, trust, and faith. Simply, thank you for being by my side. I know there is a great future waiting for us, and we will embark this journey together hand-in-hand.

TABLE OF CONTENTS

LIST OF TABLES

LIST OF FIGURES

LIST OF ABBREVIATIONS

1-, 2-, 3-D	One-, two-, three-dimensional
ABF	Adaptive bilateral filter
ACWM	Adaptive center weighted median filter
A\D	Analog-to-digital
AI	Artificial intelligent
ANFIS	Adaptive neural network-based fuzzy inference system
ANN	Artificial neural network
ASWM	New adaptive switching median filter
AVSHC	Augmented variational series and histogram-based clustering filter
BF	Bilateral filter
BK	Bilateral kernel
BLS	Bayesian least-square
BM3D	Block-matching 3-D filter
BV	Background variance
CCD	Charge-coupled device
CE	Contrast enhancement-based filter
CFA	Color filter array
CMOS	Complementary metal-oxide semiconductor

CPU	Central processing unit
CWM	Center weighted median filter
DCT	Discrete cosine transform
DCWM	Directional center weighted median filter
DFT	Discrete Fourier transform
DOF	Depth-of-field
DS-FIRE	Dual-step FIRE
DSLR	Digital single-lens reflex
DV	Detail variance
DWM	Directional weighted median filter
EM	Expectation minimization
FF-ANN	Feed-forward ANN
FIET	Fuzzy image enhancement method
FIN	Fixed-valued impulse
FIRE	Fuzzy inference ruled by else-action
FMEM	functional minimization effective median
GP	Genetic programming
GSM	Gaussian scale mixture
GUM	Generalized unsharp-masking filter
HE	Histogram equalization

HMT	Hidden Markov tree
HOG	Histogram of oriented gradients
IDE	Integrated design environment
IID	Independent and identically distributed
ISO	International Organization for Standardization
KASPR	Adaptive kernel-based semi-parametric regularization
LABC-I	Locally adaptive bilateral clustering I filter for image denoising
LABC-II	Locally adaptive bilateral clustering II filter for image enhancement
LAFSM	Locally adaptive fuzzy switching median filter
LARK	Locally adaptive regression kernel
LMS	Least mean-square
LoG	Laplacian of Gaussian
MAD	Median of absolute deviation
MAE	Mean absolute error
MIX	Mixed impulse
MR	Magnetic resonance
MRF	Markov random field
MSE	Mean-squared error
MMSE	Minimum mean-squared error
NLI	Normalized local information

NLM Non-local means filter

OSA Optimal spatial adaptive filter

PCA Principle component analysis

PC-ANN Pulse-coupled ANN

PDF Probability density function

PSF Point spread function

PSNR Peak signal-to-noise ratio

PWL-FIRE Piecewise-linear FIRE

PWMAD Pixel-wise median of absolute deviation

RGB Red-Green-Blue

RIN Random-valued impulse

RINVE Robust impulse noise variance estimation

RKHS Reproducing kernel Hilbert spaces

ROAD Rank-order absolute difference

ROLD Rank-order logarithmic difference

RORD Rank-order relative difference

SB Switching bilateral filter

SKR Steering kernel regression

SNP Salt-and-pepper

SNR Signal-to-noise ratio

SO-ANN Self-organizing ANN

SRHE Sub-region histogram equalization filter

SSIM Structural similarity index metric

SURE Stein's unbiased risk estimator

SUSAN Smallest univalue segment assimilating nucleus

SVD Singular value decomposition

TF Trilateral filter

TLIDE Triangular-based linear integration with differential evolution

TM Tri-state median

TV Total variation

UINTA Unsupervised, information-theoretic, adaptive filter

UM Unsharp-masking filter

UNIF Uniform impulse

VLSI Very large scale integration

Y-Cb-Cr Intensity, luminance, and chrominance channels

LIST OF SYMBOLS

α_i	Impulse detection switch
δ	The statistic of local dominant feature
ε	The offset function for gradient estimation
γ	The real scaling factor
λ	Mean and variance of the Poisson distribution
μ_{C_L}	The mean intensity of the largest cluster C_L
μ	The piecewise-linear fuzzy set
μ_g	Mean of the Gaussian distribution
μ_u	Mean of the uniform distribution
μ_H	The Huber influence function
σ_{C_L}	The standard deviation of intensity in C_L
σ_g	Variance of the Gaussian distribution
σ_u	Variance of the uniform distribution
σ_R	The radiometric smoothing scalar
σ_S	The spatial smoothing parameter
ρ	Impulse noise density probability
$\varphi^{(t)}$	The NLI roughness index
ξ^{-1}	Inverse operator for imaging system

a_i	General additive noise function
$a_{i,Gaussian}$	Gaussian distribution function (f_g)
$a_{i,uniform}$	Uniform distribution function (f_u)
b_i	General blurring point spread function
$B^{(t)}$	The binary noise map
c_i	The cluster of interest containing the pixel of interest i
c_j	The neighboring clusters consists of the neighboring pixels j
$\mathbf{C}_j$	The structure tensor
$C(\cdot)$	The zth cluster
C_D	The dominant cluster
C_{first}	The first cluster
C_{free}	The noise-free cluster
C_{last}	The last cluster
C_L	The largest cluster
C_{pepper}	The pepper-noise cluster
C_{salt}	The salt-noise cluster
d	The distance measure
d_w	The weighted distance measure (except for weighted Euclidean)
D	The linkage measure
D_j	The Euclidean distance between j and i pixels

f_{mix}	Mixed impulse noise function ($I_{i,MIX}$)
$f_{Poisson}$	Poisson distribution function
f_{snp}	Salt-and-pepper noise function
f_{unif}	Uniform impulse noise function
$F_1^{(t)}$	The first adaptive threshold of μ
$F_2^{(t)}$	The second adaptive threshold of μ
F_i	The fuzzy set for processing the local information
$g(\cdot)$	Horizontal or vertical image gradient
G_i	The number of noise-free pixels in $N_f(i)$
h_I	Effective area for impulse detection
h_x	Spatial variance parameter
h_{xy}	Global smoothing parameter
h_y	Intensity bandwidth parameter
HB	The upper boundary
i	The i-th pixel of interest
I_i	General impulsive noise function
I_{lower}	The lowest intensity in C_L
I_{upper}	The highest intensity in C_L
I_{max}	Maximum intensity value in the dynamic range
I_{min}	Minimum intensity value in the dynamic range

I_{pepper}	The local maximum representing the pepper-noise intensity
I_{salt}	The local maximum representing the salt-noise intensity
j	The j-th neighboring pixel
J_{ij}	The joint impulsivity
k	The first k-th sorted elements
K_p	The p-th Laplacian kernel
$K(\cdot)$	The kernel function
L	The size of local window patch
L_d	The size of local detection window
L_f	The size of adaptive local filtering window
L_I	The extracted local information
LB	The lower boundary
m	Sequence of the variational and augmented variational series
m_i	Median pixel
$M_1 \times M_2$	Image dimension
n	Sequence of the sorted pixel intensity
n_i	The number of elements in cluster c_i
n_j	The number of elements in cluster c_j
$N(i)$	The local search window
$N_d(i)$	The local detection window

$N_f(i)$	The local filtering window
$N_n(i)$	The set of neighboring pixels, known as the neighborgram
$N_s(i)$	The sorted neighborgram
$p(Y_k)$	The probability of the k-th gray level
Q	The quality parameter for image compression
r_i	Minimum Laplacian product
$\mathbf{S}$	The scatter matrix
t	The number of iteration
T_1	The first threshold defining the shape of the fuzzy set F_i
T_2	The second threshold defining the shape of the fuzzy set F_i
T_c	The clustering threshold
T_s	The switching threshold
T_V	The scaling factor
$\mathbf{v}$	The augmented feature vector
V	The variational series
V_m	The augmented variational series
$\mathbf{V}_j$	Local noise variance
$\mathbf{w}$	The weight function
w_i	Individual weight for weighted averaging filters
w_m	Repetitive weight for weighted median

w_x	The spatial weight coefficient
w_y	The photometric weight coefficient
w_r	The spatial similarity kernel for the BF
w_R	The spatial similarity kernel for the proposed bilateral clustering
w_s	The radiometric similarity kernel for the BF
w_S	The radiometric similarity kernel for the proposed bilateral clustering
w_S^I	The vectorially indexed w_S
x_i	The spatial position of the pixel of interest
x_j	The spatial positions of the neighboring pixels
x_s	The vectorially indexed spatial position
y_i	The intensity of the pixel of interest
$y_{i,lowpass}$	The output of a lowpass filter
y_j	The intensities of the neighboring pixels
$\mathbf{y}_i$	Group of intensities within the patch of the pixel of interest
$\mathbf{y}_j$	Group of intensities within the patch of the neighboring pixels
$\widetilde{y_i}$	The estimate of y_i
$\widetilde{y_{bi}}$	The estimate of y_i using the BF
$y_{i,n}$	The intensity of the i-th pixel in the noisy image
$y_{i,o}$	The intensity of the i-th pixel in the original image
y_s	The sorted pixel intensity

Y_k	The k-th gray level
z	The number of cluster

RANGKA KERJA TEGUH UNTUK NYAHHINGAR DAN NYAHKABUR IMEJ BERDIGIT

ABSTRAK

Pemulihan imej adalah pendekatan untuk meningkatkan visual kualiti imej yang ditangkap agar kualitinya lebih baik daripada had kualiti kamera. Kemajuan dalam teknologi pengimejan dan multimedia telah menonjolkan kepentingan pemulihan imej menggunakan perisian termasuk aplikasi-aplikasinya dalam pelbagai bidang fotografi pengguna serta industri. Walaubagaimanapun, imej yang ditangkap sering mengalami degradasi, seperti kabur, hingar, artifak-artifak tidak diingini, dan sebagainya, akibat kekangan sistem pengimejan. Walaupun banyak usaha telah dibuat untuk meningkatkan keupayaan kaedah-kaedah sedia ada, namun, kaedah-kaedah ini masih perlahan dari segi pemprosesannya dan kebanyakannya hanya direkabentuk untuk memproses model degradasi tertentu sahaja. Oleh itu, kaedah-kaedah yang sedia ada biasanya gagal apabila diaplikasikan pada imej sebenar. Berdasarkan motivasi ini, satu rangka kerja teguh telah dicadangkan untuk menangani isu-isu utama yang berkaitan dengan masalah merekabentuk kaedah-kaedah pemulihan imej yang praktikal, iaitu, isu pemulihan kualiti visual serta kerumitan pengiraan. Ciri-ciri yang menonjolkan kelebihan rangka kerja ini adalah: (1) rangka kerja yang dicadangkan adalah teguh dalam menguruskan kehadiran ketidakpastian dalam data, (2) ia mampu menyesuaikan keadaan ruang secara setempat berdasarkan data radiometrik imej, dan (3) ia adalah sangat teguh dalam menguasai maklumat struktur setempat walaupun imej tersebut dicemari hingar. Berdasarkan kelebihan rangka kerja teguh ini, tiga kaedah pemulihan imej baharu telah dilaksanakan dalam penyelidikan ini. Kaedah pertama, yang digelar “Augmented Variational Series and

Histogram-based Clustering” (AVSHC), adalah penuras skim pensuisan yang mampu untuk menapis hingar impuls dalam imej warna atau monokrom. Kemudian, dua variasi penuras yang berdasarkan kaedah teguh “Locally Adaptive Bilateral Clustering” (LABC) telah dicadangkan untuk nyahhingar, nyahkabur sederhana, dan menyerlahkan ketajaman imej. Variasi pertama, iaitu penuras LABC-I, mampu untuk menapis hingar tambahan, impuls, dan campuran kedua-dua jenis hingar; manakala variasi kedua, penuras LABC-II, mampu untuk menyingkirkan artifak-artifak kabur dan hingar, serta pada masa yang sama, meningkatkan ketajaman imej yang telah dibaikpulih. Oleh kerana rangka kerja teguh ini tidak bergantung kepada sebarang andaian spesifik mengenai model isyarat dan hingar, penuras-penuras yang berasaskan rangka kerja ini boleh digunakan untuk pelbagai masalah pemulihan imej, seperti nyahhingar, nyahkabur, meningkatkan ketajaman imej, dan sebagainya. Ini membuktikan keteguhan rangka kerja yang telah dicadangkan. Tambahan pula, keputusan uji kaji yang menggunakan imej-imej simulasi dan sebenar bagi ketiga-tiga kaedah yang dicadangkan menunjukkan prestasi pemulihan yang baik dari segi visual mahupun kuantitatif. Kelebihan pada "peak signal-to-noise ratio" (PSNR) dan "mean-absolute error" (MAE) menonjolkan kebolehan penuras-penuras yang dicadangkan mengatasi beberapa kaedah terdahulu dalam kajian ilmiah. PSNR yang lebih tinggi menunjukkan penindasan hingar yang lebih baik, manakala MAE yang lebih rendah mendedahkan ciri pemeliharaan terperinci kaedah-kaedah yang dicadangkan. Di samping itu, visual yang menarik bagi pemulihan imej-imej sebenar yang dicemari turut menekankan kepentingan penuras-penuras yang dicadangkan untuk aplikasi sebenar. Selaras dengan reka bentuk peralatan pengimejan moden, penuras-penuras yang telah dicadangkan mempunyai implementasi yang mudah dan pelaksanaannya adalah laju secara relatif.

ROBUST FRAMEWORK FOR DIGITAL IMAGE DENOISING AND DEBLURRING

ABSTRACT

Image restoration concerns improving visual quality of a captured image that goes beyond the achievable limit of camera. Recent advancement in imaging and multimedia technology has advocated the interests of image restoration through software, of which applications permeate consumer photography as well as different industries. Unfortunately, the captured images often suffer from degradations, such as blurring, noise, unpleasant artifacts, and more, due to limitations of the imaging system. Despite considerable efforts have been channeled to advance the state-of-the-art methods, surprisingly, these methods are often slow and only designed for handling specific degradation model. As such, the existing methods usually fail when applied to degraded real images. Based on this motivation, a robust framework is proposed to address the main issues related to designing practical image restoration methods, namely, visual restoration quality and computational complexity. The robust framework has several advantageous properties: (1) the proposed framework is robust towards the presence of data uncertainties, (2) it is spatially adaptive to the radiometric structures of the image data, and (3) it is exceedingly robust in capturing the local structural information even in noise-ridden images. By capitalizing on the advantages of this robust framework, three novel image restoration methods have been developed in this work. The first method, termed as Augmented Variational Series and Histogram-based Clustering (AVSHC), is a switching-scheme filter that is capable to remove any kind of impulsive noise on color or monochrome images. Then, two variants based on a robust method, called Locally Adaptive Bilateral Clus-

tering (LABC), are proposed for image denoising, mild deblurring, and sharpness enhancement. The first variant, i.e., the LABC-I filter, eliminates additive, impulsive, and mixed noise; whereas the second variant, LABC-II filter, removes blur and noise artifacts, at the same time, increases the sharpness of the restored image. Because the robust framework does not rely upon any specific assumptions about the signal and noise models, the filters derived from the framework are applicable to a wide variety of image restoration problems, such as denoising, deblurring, sharpness enhancement, and more. This demonstrates the robustness of the proposed framework. Furthermore, extensive experimental results from real and simulated image data show the proposed filters are capable to achieve excellent restoration performance, both quantitatively and visually. Their excellent peak signal-to-noise ratio (PSNR) and mean absolute error (MAE) beckons the superiority of the proposed filters over some well-known methods in the literature. The higher PSNR manifests their good noise suppression strength while the lower MAE reveals their detail preservation characteristic. On another front, attractive visual appeal in the restoration of degraded real images further underlines the importance of the proposed filters for real applications. In line with the design of modern image-capturing devices, the proposed filters have simple and straightforward implementation that results in relatively fast runtime.

CHAPTER 1

INTRODUCTION

1.1 Preliminaries

With recent advancement in imaging technology, image restoration has found renewed interest among image capturing device manufacturers and researchers. The past few years have witnessed an explosion in the availability of photographic data from multiple image capturing devices. For example, cell-phone cameras and commercial digital cameras are the common sources for imagery data which rapidly gaining consumer acceptance. To keep up with rising demands for high resolution imaging devices, more image sensors are packed on a chip. Unfortunately, image capturing devices become increasingly sensitive towards the exposure of noise as the number of pixels per unit area grows. Higher pixel densities embedded in image capturing devices and faster shutter speeds result in blur and noise in the captured image [1]. As a cost effective and economical alternative, the captured image is processed by image restoration (e.g., deblurring, denoising, sharpening, etc.) algorithms to recover the high quality original image [2].

Generally, noise characteristics in an image depend on many factors including sensor type, temperature, and various camera settings (e.g., aperture size, exposure time, and the International Organization for Standardization (ISO) speed) [3]. In real applications, particularly consumer digital imaging, it is common to record weakly blurred and relatively noisy images. Simpler image capturing devices, e.g., camera phone, tend to produce noisier image due to physical limitations such as fixed-focus lenses and smaller image sensors. In addition,

limited accuracy of auto-focusing systems and photon-limited low-light condition may add extra blur and noise into the image. Besides, other probable causes of image noise include faulty memory units, external disturbances in noisy environments, and compression errors.

In digital imaging, the captured noisy image is preprocessed and restored in the early pipeline of image formation before subsequent image processing tasks are carried out. Apart from the obvious visual improvement in the restored image, image restoration is imperative, and even indispensable, because the accuracy of subsequent operations (such as image classification, segmentation, parameter estimation, etc.) is largely affected by the quality of the restored image. Furthermore, the application of image restoration technology vastly stretch over, but are not limited to:

- *Consumer electronics and industrial applications*: Designing economical digital cameras, scanners, and image-based instruments.
- *Scientific imaging*: Enhancing images from telescopes (astronomy), electronic or optical microscopes (biology), medical imaging equipments (medicine), and spectroscopy (remote sensing).
- *Information forensics and security*: Enhancing images from surveillance cameras and biometric systems.

Roughly speaking, image restoration is a very basic problem that is computationally complex and mathematically ill-posed. All this makes image restoration an interesting research avenue for the image processing and computer vision communities to pursue.

1.2 Image Restoration: Direct Model and Inverse Problem

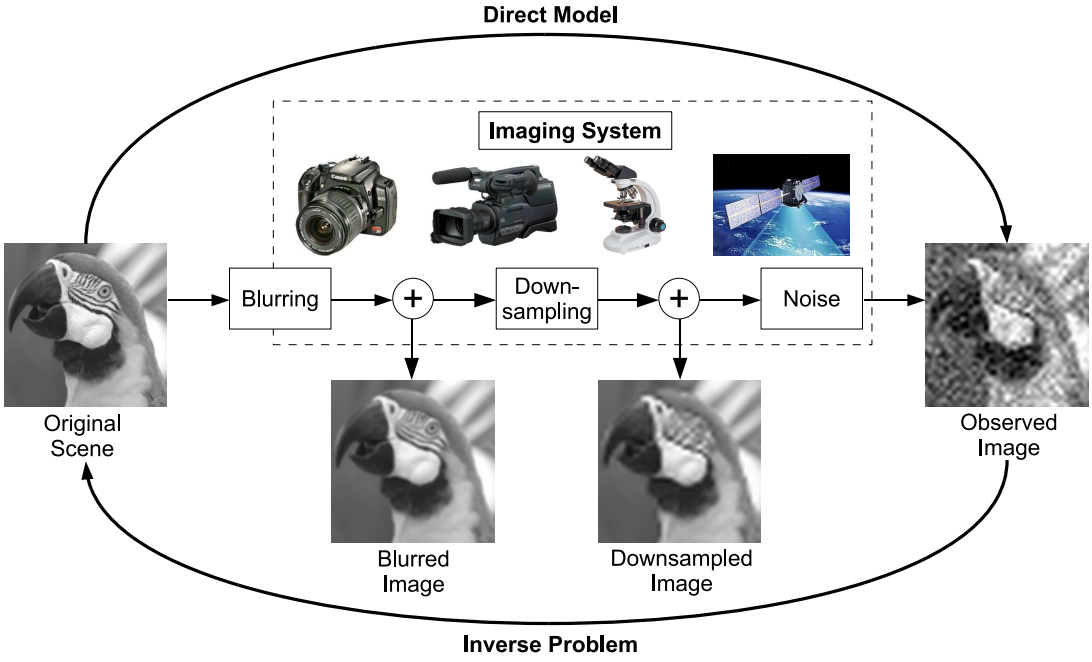

Figure 1.1: A block diagram representation of a typical digital imaging system. The direct model is a mathematical description of the image formation pipeline. The inverse problem is the process of recovering the original scene from the noisy observed image.

Image restoration attempts to recover the original, high-frequency image which is subjected to the degradation of an imaging system. Such problem is an example of inverse problem, wherein the information (original image) is estimated from the observed data (noisy image) using image restoration algorithms. However, solving the inverse problem requires first formulating the direct model [4]. Undoubtedly, the most common direct model representing image degradation process can be interpreted as that of computing the noisy observation pixel intensity y_i from the noise-free pixel intensity $\widetilde{y}_i$ at the position i where

$$y_i = [(\widetilde{y}_i \otimes b_i) + a_i]I_i. \tag{1.1}$$

Here, $\otimes$ is the convolution operator, whereas a_i, b_i, and I_i represent the additive, blurring, and impulsive degradation processes, respectively, as illustrated in Figure 1.1. In conjunction

with image restoration, these degradation processes allow image restoration algorithms to be flexibly formulated. However, before the development of these algorithms can be performed, it is crucial to understand the characteristics of the corrupting noise. To do so, the next section is dedicated to study the properties and sources for a_i, b_i, and I_i.

1.3 Image Noise and Degradation Processes

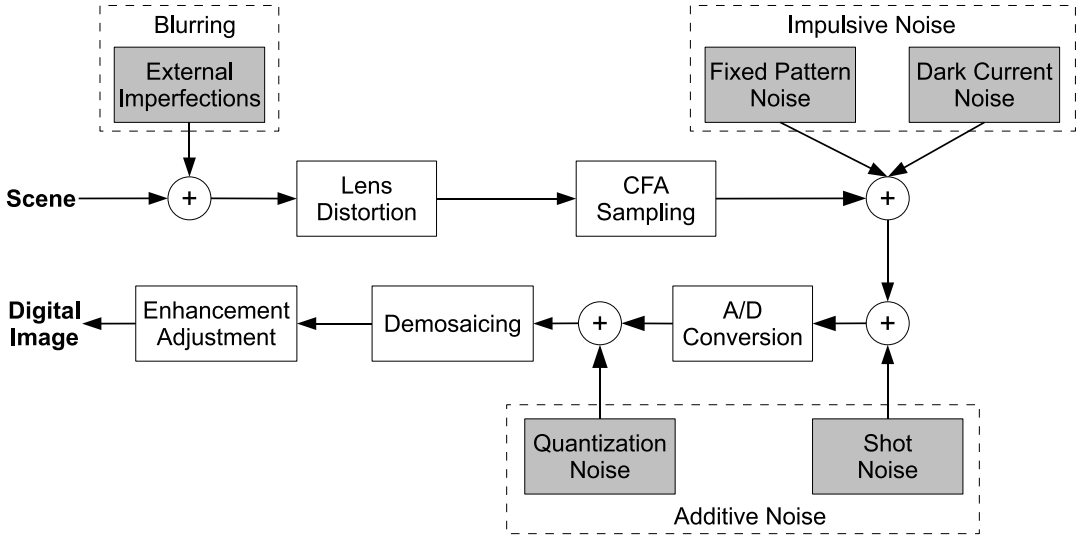

Figure 1.2: A canonical image formation model with the various noise sources (adapted from [5]). These noise sources are categorized as additive, impulsive, or convolutive (blurring).

In the simple image formation pipeline shown in Figure 1.2, incident light rays from the scene entering the lens of the camera are unevenly focused on the camera sensors regardless of the sensor type, be it the kind with charge-coupled device (CCD) or complimentary metal-oxide semiconductor (CMOS) technology. The geometrically distorted light rays then undergo various processing stages. A color filter array (CFA), in which each sensor element responds to a distinct range of light wavelengths, accumulates and converts the reaching light rays, or photons, to electrical signal that is then read and stored as digital information. Subsequently, demosaicing is performed to interpolate incomplete color information at each pixel location in the CFA. Towards the end of the image capturing process, further image enhancement

adjustments (e.g., color-tone mapping, gamma correction, and white balancing) are carried out before the final image is produced [5].

Noise corrupting the final image is introduced in various stages during image acquisition (see Figure 1.2). The distortion caused by lens due to its non-uniform response to light rays generates the fixed pattern noise. Simultaneously, dark current noise appears due to anomalous charges present at the image sensors even without any incident photon [6]. Then, thermal noise develops due to the heating of electronic circuitry of the camera in use [7]. By far, this noise increases with the duration of use. During the signal analog-to-digital conversion, quantization noise may arise as a result of insufficient number of bits to hold the pixel information [5]. Unlike the aforementioned noise, the origin of the corrupting shot noise is independent of any physical limitation in the imaging system. In fact, shot noise is caused by the photonic nature of light itself and, hence, the captured image always appears noisy. Besides, external disturbances, such as atmospheric disturbances, camera or object motions, etc., cause the image to appear blurry.

For a given camera, these noise sources can be effectively modeled and, thus, controlled. For instance, quantization noise can be alleviated by adequately choosing sufficient number of bits to avoid truncating the image signals. With respect to the linear direct model in (1.1), fixed pattern noise and dark current noise are modeled as impulsive noise I_i in the resultant image. On the other hand, shot noise and quantization noise are modeled as additive noise a_i, while blurring is modeled as a shift-invariant, convolutive point spread function b_i. Therefore, the direct model in (1.1) is also referred as the linear, shift-invariant degradation model [8]. In the following subsections, an attempt to study and understand the characteristics of a_i, b_i, and I_i is pursued in great depth.

1.3.1 Impulsive Noise and its Properties

Consider an image of size $M_1 \times M_2$ stored as 8-bit grayscale pixel resolution, pixel intensities lie in the dynamic range $[I_{min}, I_{max}]$, where I_{min} and I_{max} represent the lowest and highest intensities, respectively. Regardless of its origin, impulse noise randomly misfire a certain percentage of pixels with intensity values significantly different from the uncorrupted neighborhood. Based on this fact, an image contaminated with impulse noise of probability[1] ρ can be modeled as:

$$I_i = f(y_i) = \begin{cases} y_{i,n} & : \text{ with probability } \rho, \\ y_{i,o} & : \text{ with probability } 1-\rho, \end{cases} \tag{1.2}$$

where $y_{i,n}$ and $y_{i,o}$ represent *i*-th pixel intensity of the noisy and original images, respectively.

Fundamentally, there are two types of impulse noise models widely used in image processing literature: the random-valued impulse noise (RIN) model and the fixed-valued impulse noise (FIN) model. The former is also known as the uniform impulse (UNIF) noise and noise pixels can take any intensity values within the image dynamic range, i.e., $f_{unif}(y_i) \in [I_{min}, I_{max}]$. Alternatively, the FIN model assumes a limited number of impulsive intensities that appear in certain percentages, for examples, see [9, 10]. On a related note, the simplest and most frequently used FIN model in contemporary literature is the salt-and-pepper (SNP) noise. Under the assumption of the SNP noise model, impulsive pixels are assumed to take the minimal and maximal intensities, i.e., $f_{snp}(y_i) \in (I_{min}, I_{max})$.

In reality, *a priori* knowledge on the impulsive amplitudes and the impulse noise densities are neither known in advance nor can be precisely estimated. In fact, impulse noise is resulted from interference of noise signals with arbitrary amplitudes. Consequently, the im-

[1] Impulse noise probability is also known as impulse noise density. Both refer to the percentage of corrupted pixels, and these two terms are used interchangeably in literature.

pulsive amplitudes could either fall inside or outside of the image dynamic range. When the impulsive amplitude lies within the image dynamic range, the corresponding pixel appears as UNIF noise in the noisy image. On the other hand, if the impulsive amplitude falls outside of the image dynamic range, the corresponding pixel is saturated and flipped to the maximal or minimal intensity and emerges as SNP noise. Under these circumstances, it is appropriate to consider a more general impulse noise model.

Apparently, real impulse noise is some mixture between the SNP and UNIF noise models. For this reason, the authors in [11] have proposed a simplified but realistic impulse noise model that contains both the SNP and UNIF noise models. The general impulse noise model, called the mixed impulse (MIX) noise, is given here as:

$$I_{i,MIX} = f_{mix}(y_i) = \begin{cases} f_{unif}(y_i) & : \text{ with probability } 0.5\rho, \\ f_{snp}(y_i) & : \text{ with probability } 0.5\rho, \\ y_{i,o} & : \text{ with probability } 1-\rho. \end{cases} \tag{1.3}$$

In this way, half of the impulsive pixels are modeled as SNP noise while the remaining half as UNIF noise. If impulse noise in image degradation is thought of as a combination of two independent processes of injecting the image with f_{snp} and f_{unif}, the question of choosing an appropriate impulse noise model boils down to the selection of the MIX noise model. As a result, this work advocates the use of MIX noise model in (1.3) because it is deemed more suitable and reasonable when testing the performance of impulse noise filter. To show the severity of impulse noise corrupting images, Figure 1.3 illustrates the test image added with the SNP, UNIF, and MIX impulse noise.

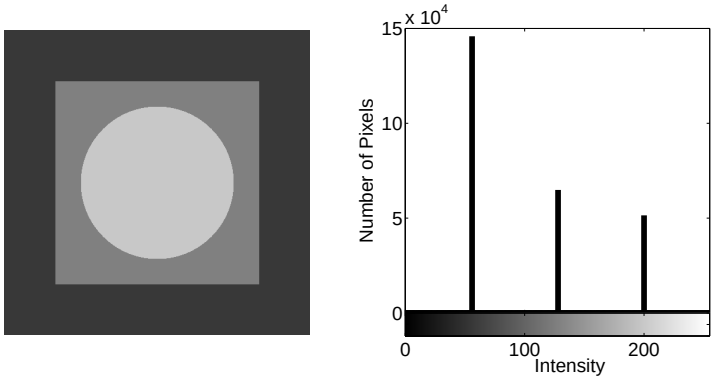

(a)

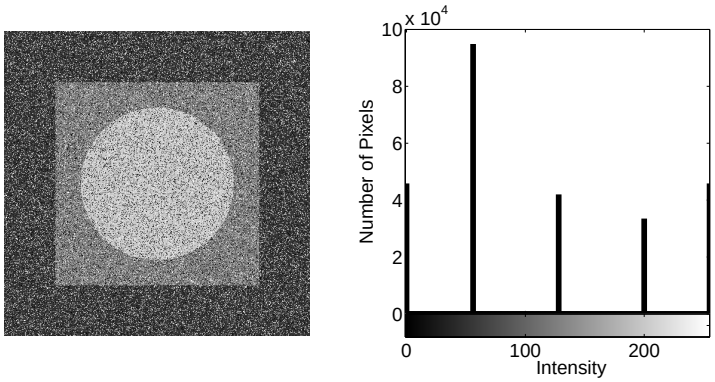

(b)

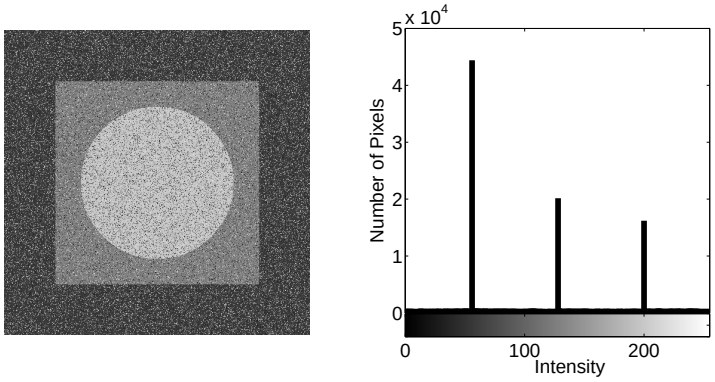

(c)

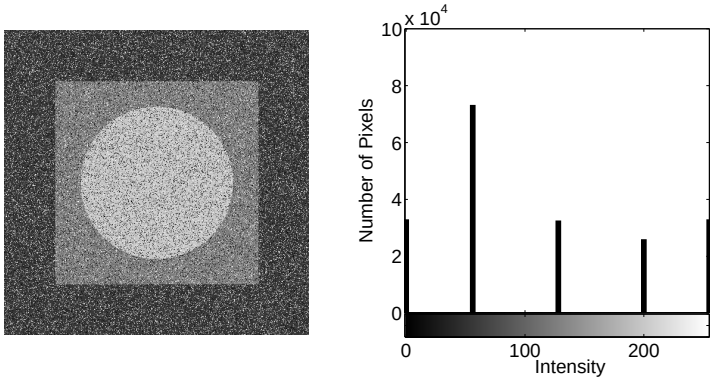

(d)

Figure 1.3: (a) The original test image and its histogram. Images corrupted by (b) SNP, (c) UNIF, and (d) MIX impulse noise, and their respective histograms.

1.3.2 Additive Noise and its Properties

Additive noise in the captured image is typically modeled as Gaussian distributed probability density function (PDF), although the noise source normally gives rise to Poisson PDF. As for the case of shot noise, photons do not necessarily hit the image sensors evenly despite the scene is homogeneous.[2] This photon counting process, which can be described by the Poisson distribution with mean and variance λ

$$f_{Poisson}(y_i;\lambda) = \frac{\lambda^{y_i}\exp(-\lambda)}{y_i!}, \tag{1.4}$$

is signal-dependent and causes the resultant image to appear "grainy." Under low-light condition, the noise has significant dominance in the captured image when limited photons are available to the image sensors. Conversely, when a large number of photons present in the image sensors, i.e., the image is well-exposed, the Poisson PDF closely resembles the Gaussian PDF. Moreover, variance stabilization methods, such as Anscombe root transformation [12], can be used to approximate a Gaussian distributed PDF for any given image signal with Poisson PDF. Furthermore, the photons reaching each image sensor are accumulated independent of the neighboring sensor elements and they can be assumed to be spatially uncorrelated [7]. For this reason, shot noise in image is popularly modeled as independent and identically distributed (IID) and zero-mean additive white Gaussian noise (AWGN), given as [13]

$$a_{i,Gaussian} = f_g(y_i;\mu_g,\sigma_g^2) = \frac{1}{\sqrt{2\pi\sigma_g^2}}\exp\left[\frac{-(y_i-\mu_g)^2}{2\sigma_g^2}\right], \tag{1.5}$$

where μ_g and σ_g^2 are the mean and variance, respectively, of the Gaussian distribution.

[2] It is worth noting that a single noise in the captured image could have numerous names under different circumstances. For example, shot noise in the imaging system is mathematically represented by Gaussian (or Poisson) distribution in image restoration. Since the mathematical modeling of Gaussian noise is characteristically additive in nature (referring to (1.1)); thus, shot noise modeled as Gaussian noise also falls under the category of additive noise.

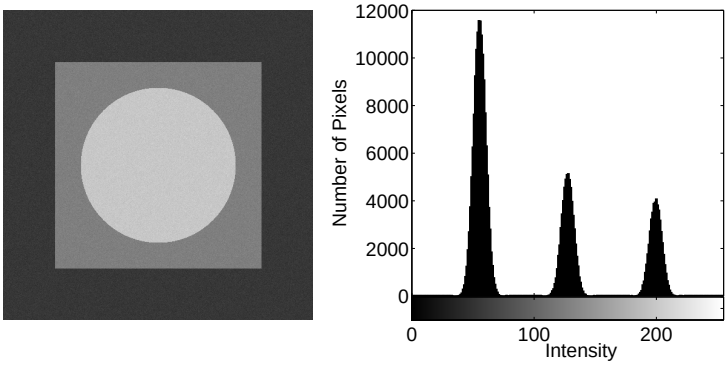

(a)

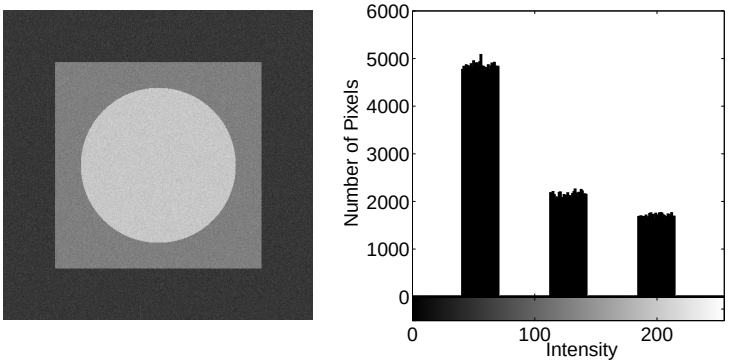

(b)

Figure 1.4: The resultant test images added with (a) Gaussian and (b) uniform noise. The histograms indicate the characteristics of the corresponding noisy images.

Another form of additive noise commonly addressed in image processing literature is the uniform noise. As illustrated in Figure 1.2, quantization noise in imaging system can be approximately modeled as uniform noise. The intensity truncation of the sensed image signals into a number of discrete levels caused the PDF to appear being “clipped." Basically, the process is stochastic and signal dependent, unless the presence of other noise sources that are strong enough to cause dithering will turn it to become signal independent. The uniform PDF with mean μ_u and variance σ_u^2 is given in parametric form by [13]

$$a_{i,Uniform} = f_u(y_i;\mu_u,\sigma_u^2) = \begin{cases} \frac{1}{\sqrt{12\sigma_u^2}} & : \quad \mu_u - \sqrt{3\sigma_u^2} \le y_i \le \mu_u + \sqrt{3\sigma_u^2}, \\ 0 & : \quad \text{otherwise.} \end{cases} \tag{1.6}$$

As an example, Figure 1.4 illustrates the two types of additive noise, i.e., Gaussian and uniform noise, corrupting the test image.

1.3.3 Mixed Noise and its Relevance in Real Image Degradation Process

Having seen the noise degradation sources in an imaging system, it is apparent that the corrupting noise within the internal imaging pipeline will result in a final image degraded with a mixture of both additive and impulsive noise. Considering this fact, a practical way for simulating real image noise is to blend together both additive and impulsive noise, for example, the Gaussian or uniform noise is fused with the MIX impulse noise. In this way, noise filter can be reasonably tested and the results obtained speak volume of its performance when brought to real-world applications. Figure 1.5 shows examples of mixed noise corruption in scathing the appearance of the test image.

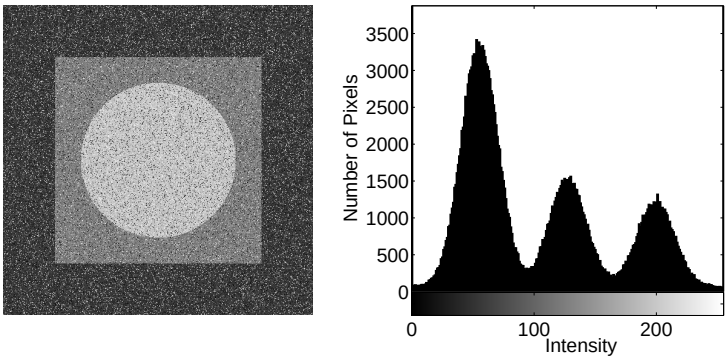

(a)

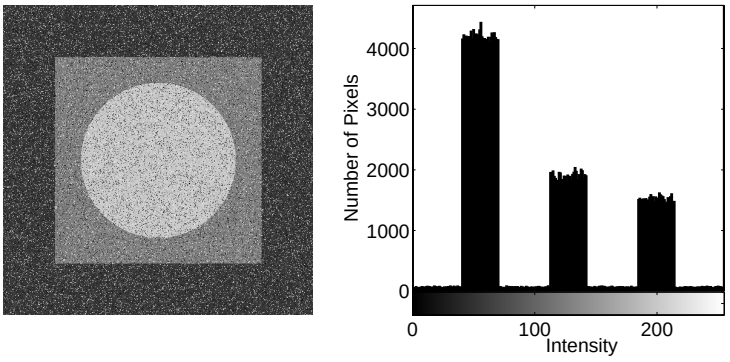

(b)

Figure 1.5: Examples on mixed noise corruption. (a) Gaussian noise plus MIX impulse noise. (b) Uniform noise plus MIX impulse noise.

1.3.4 Image Blurring

Blurring of digital image is a problem caused by some imperfections encountered outside of the imaging system during image acquisition. For example, the blurring in aerial photographs is due to atmospheric turbulence and relative motions between the camera and the ground [14]. In consumer digital photography, the digital single-lens reflex (DSLR) camera setting plays an important role that strongly affect the sharpness of the captured image [15]. On the other-hand, limited accuracy and error under auto-focus camera setting may add extra blur into the captured image.

Specifically for digital camera, given a fixed exposure time, a large aperture size will result in image with higher signal-to-noise ratio (SNR), i.e., the captured image is less noisy. However, the depth-of-field (DOF) will be lowered and, thus, introducing the out-of-focus blur. Conversely, a small aperture size will mitigate the blur but, at the same time, increases the noise level as well. On the contrary, using longer exposure time may relieve both noise and out-of-focus blur; nevertheless, such setting may cause camera or object motions blur, which is even more difficult to eradicate [15].

In general, image blur can be effectively modeled by mathematically convolving a shift-invariant point spread function (PSF), b_i, with the noiseless image signal $\widetilde{y_i}$. The PSF acts as a low-pass filter to smooth image details. As an example, the version of the blurred test image is shown in Figure 1.6. Interestingly, while image deblurring remains as an active research domain for the image processing community, image blurring is also used as a powerful tool in various graphics and image editing software, typically for improving image aesthetic quality by emphasizing on the artistic *bokeh* effect.

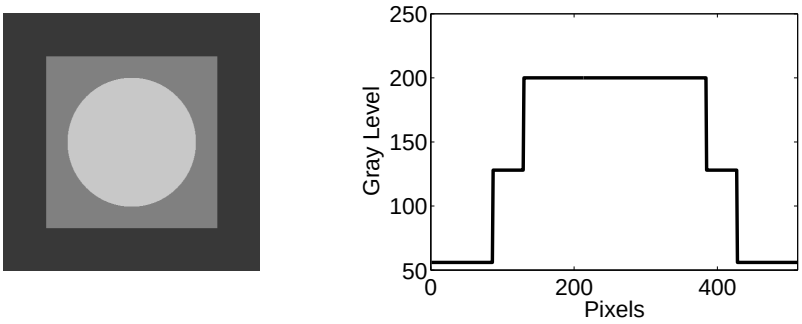

(a)

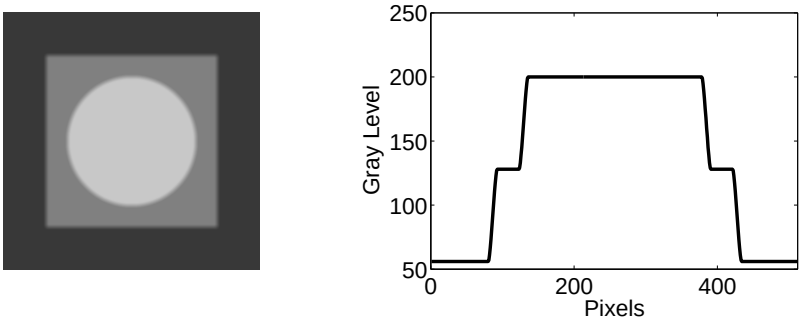

(b)

Figure 1.6: (a) The sharp test image and its edge profile from the horizontal cross-section of the image through its center point. (b) The blurred test image smoothed by a circular PSF. Note that nearby pixels along sharp edges are redistributed and formed ramp slopes in the edge profile of the blurred image.

1.4 Problems and Motivation

An inherent complication with inverse problems, as the name suggests, is the difficulty in inverting the direct model without amplifying the noise in the observed image. This point is illustrated by a practically clean but naive deconvolution estimate [16]

$$\widetilde{y_i} = \xi^{-1} y_i = [y_i + (a_i b_i^{-1})] I_i^{-1}, \tag{1.7}$$

where ξ^{-1} is the inverse operator of the imaging system in Figure 1.1, assumed to be linear and time-invariant. Unfortunately, the variance of the $a_i b_i^{-1}$ noise term is large and ill-conditioned. As a consequence, the solution is neither unique (singular) nor it exists for arbitrary data; thus, making $\widetilde{y_i}$ an unsatisfactory estimate for y_i. Moreover, the challenge of inverting the direct model is exacerbated by the fact that the solution is highly sensitive to the

I_i^{-1} impulsive noise term, which is random in nature.

By looking at a broader picture, the problems plaguing image restoration methods share the same root as those of the inverse problems. In filter design, these problems are mainly rooted in the solution that uses linear combination of local data as an approximate for the original scene. This estimate is no doubt elegant, relatively easy to analyze, and have attractive asymptotic properties; however, such estimation is also prone to error due to the nonlinear behavior of noise. At best, the restored image would contain a minimal amount of undesirable noise effects. At worst, the integrity of the information represented by minute details and sharp edges are either damaged or missing. This research acknowledges such flaw and the design of the proposed methods takes into account this limitation. For instance, this problem can be remedied by introducing an adaptive clustering approach for selectively choosing the “useful" photometric (intensity) and spatial data for restoration.

Aside from the inheritance problems, nonadaptive data kernel, be it the kernel support size or shape, leads to a more pronounced restoration problem. Image restoration methods should not rely on only the pixel photometric properties and noise densities, but also on the sample location. In any case, breaking the bilateral photometric and spatial relation limits the degrees of freedom since the correlation between pixel spatial position and its photometric intensity is ignored. Clearly, this weakens the performance of the filter. In other words, the effective kernel size and shape should be locally adapted to image features such as fine details, edges, and textures. In what follows, a solution is proposed to overcome this drawback by using a “soft" approach. The restoration term is computed based on the combination of bilateral (photometric and spatial) weights in order to have a more effective and nonlinear action on the data. The outcome is an equivalent steerable kernel adapted to the local image features.

Ultimately, the grand challenge in image restoration is in designing a robust framework capable for filtering various noise types. Over the years, a great number of methods targeting only a particular noise have been proposed, leading to a cacophony of filters including some well-known approaches in image restoration. At large, competent filters for impulsive denoising would fail completely when used for additive noise removal, and vice versa; leave alone the more complicated scenario involving image deblurring. Moreover, some of the existing methods are impractical for real-world application in the sense that they are computationally expensive. The runtime consumption ranges from a mere fraction of second and up to few hours long, with the latter being considered as extremely slow under the modern standard of consumer-based image applications [17].

Owing to the abovementioned drawbacks, this research is motivated to develop a “universal" framework for fast and robust image restoration. In this research, many image restoration problems frequently encountered in real imaging systems, such as additive and/or impulsive denoising, image deblurring, and sharpness enhancement, are all addressed within a common framework. The main idea behind the proposed approach is based on adaptive clustering of locally augmented signal with the aid of soft-computing techniques.

1.5 Research Objectives

The content of this research reflects the goals it intends to accomplish. The specific objectives envisioned for this work are as follows:

- To propose a robust framework for restoration of linear, shift-invariant degraded images.
- To devise a high accuracy impulse detector and an adaptive filter for impulse detection and reduction.

- To develop a fast and robust technique for additive and mixed noise filtering.
- To design an integrated algorithm for mild image deblurring and sharpness enhancement.

As opposed to the multitude of methods in literature that only manifest themselves in a particular noise distribution, this research proposes a common framework to address the different types of noise introduced in various stages within or outside of the canonical image formation pipeline (q.v. Figures 1.1 and 1.2). Primarily, this research is made up of three main parts. The first part is dedicated to impulsive noise filtering, in which a filter is devised for color and grayscale image denoising. The second part is centered on developing a fast and robust method based on bilateral clustering for additive and mixed noise reduction. In the third part, the research extends the bilateral clustering approach to propose an algorithm for mild image deblurring and sharpness enhancement. In general, these three parts stand on a common groundwork, which is the adaptive clustering of locally augmented image signal.

Concisely, the proposed common framework is robust and universal in the sense that it can be easily manipulated to flexibly suit the type of restoration desired with minimal computation. Such ability is achievable through the design that assumes the types of noise it seeks to remove are IID and zero-mean noise. This assumption points to the worthiness that allows image restoration algorithms to be freely designed and formulated without restriction. As mentioned earlier, the proposed approach based on adaptive clustering has the advantage to segregate local image features and noise into separate clusters. As such, useful information provided by the dominant cluster can be selectively utilized for computing the estimate of noisy data. Additionally, the signal augmentation process indulges in soft-computing in an attempt to ease the difficulties encountered when dealing with uncertainties in noisy image data. To sum things up, the outcome is a framework with excellent local signal adaptation and great

immunity towards noise.

With the ever increasing demand for fast and versatile filtering techniques, this work is in parallel with the new design requirements for multipurpose image restoration (e.g., “on-the-spot" image editing software) algorithms in image capturing devices. Furthermore, the increasing number of image sensors coupled with the shrinking sensor size render a noisier captured image due to limited photons present at each sensor element. Hence, this work, which specializes in image restoration, has become even more relevant and worthwhile.

1.6 Research Scope

The scope of this research is confined to the design and development of image restoration algorithms. It begins with a meticulous literature review on various image restoration methods in an effort to understand the advantages and limitations that exist in those methods. Successively, the research then proposes image restoration algorithms that are capable to overcome the identified limitations. These proposed methods are ideal for suppressing noise and improving detail appearance, with heavy emphasis given to their practical applications. Particular attention is placed on denoising of additive (Gaussian and uniform distributions), impulsive (SNP, UNIF, and MIX models), and mixed (e.g., Gaussian plus MIX, etc.) noise. In addition, this research also focuses on mild image deblurring and sharpness enhancement. In this respect, the proposed methods only deal with images that are appropriate for digital photography; thus, images that are severely degraded are beyond the scope of this research and will not be considered.

While optics and hardware-based research are also bent on improving the visual appearance of image, this research concentrates on software-based restoration approaches, which is more popular, device-independent, and widely applicable [18]. The proposed al-

gorithms, alongside with numerous image restoration algorithms, are coded in C/C++ using Code::Blocks v8.02 integrated design environment (IDE) software, and compiled using Borland C++ v5.5 code compiler. Additional image analysis are carried out using the MATLAB® R2008a v7.6 software package. Finally, the feasibility of the proposed algorithms are demonstrated through a series of experiments. The effectiveness and applicability of the proposed methods are tested qualitatively and quantitatively using both real and synthetic image data. Simulations results obtained are visually compared and numerically evaluated using some well-known image quality metrics.

1.7 Thesis Outline

The outline of this thesis is structured as follows:

- **Chapter 2 - Literature Review**

  In this chapter, a coherent and comprehensive state-of-the-art account on recent image restoration techniques is presented. It offers an in-depth treatment of prevalent subject matters popularly discussed in image processing literature. The advantages and limitations of these methods are reviewed to gain a deeper understanding on their conceptual successes and shortcomings. In addition, image clustering is briefly reviewed for an insight into its theoretical and methodological fundamentals.

- **Chapter 3 - Clustering-Based Impulse Detection and Denoising**

  This chapter deals with impulse noise detection and reduction. Initially, a detailed description on the importance and usefulness of signal augmentation is given. Signal augmentation incorporating soft-computing is shown to alleviate the problem in thresholding and, hence, improves the accuracy in impulse detection. Consecutively, impulse detectors founded on locally augmented signal clustering and histogram-based clus-

tering are introduced. Based on the switching concept, a novel impulse filter, which is applicable to both grayscale and color images, is proposed. Additionally, a fast and accurate stopping criteria for iterative impulse denoising is developed. Experimental results are then analyzed, compared, and discussed.

- **Chapter 4 - Bilateral Clustering for Image Denoising**

  Here, a new denoising method is introduced for the removal of mutually any type of noise. Upon clustering, the clustered pixels are mapped onto a higher dimensional space with respect to the bilateral similarity kernel functions. That is to say, each pixel carries the photometric and spatial similarity measures on top of their intensity and positional values. This clustering approach is also used to demonstrate the effectiveness in providing a platform that is resilient against the effects of outliers and noise. A string of experiments is then performed by testing the proposed method with simulated and real image data. Simulation results obtained are compared with those from the state-of-the-art methods. Some implementation aspects and ways to accelerate its runtime are also briefly discussed.

- **Chapter 5 - Bilateral Clustering for Integrated Image Enhancement**

  Extending the knowledge on bilateral clustering, a robust method is formulated for joint image deblurring and sharpness enhancement in this chapter. Since the formulation is established from the key ideas in the proposed clustering approach, this method is found to be resistant to noise effects. The deblurred and/or enhanced image does not contain undesirable noise artifacts. At the end of Chapter 5, a comparative study on the performance of each method is conducted based on their simulation results. The simulation includes degraded real image data, such as out-of-focus blurred images acquired from consumer camera and blurry scanned text images.

- **Chapter 6 - Conclusion and Future Work**

  Finally, the last chapter draws the conclusions and highlights the contributions of this research. A number of interesting directions to be pursued are detailed as future works.

CHAPTER 2

LITERATURE REVIEW

2.1 Introduction

Image restoration has been a convergence of powerful ideas across a number of different disciplines such as applied mathematics, computational photography, graphics, machine learning and vision, non-parametric statistics, and signal processing. A demanding yet stimulating undertaking of image restoration algorithms is to suppress noise staining while preserving and, if possible, enhancing finer details and textures in the image. These contradictory goals have led to many different methods being proposed, with the earliest publications on the subject dated as far back as 1960s [19, 20]. Over the years, there still exists a need for the advancement of image restoration algorithms, either via proposing new approaches or by improving the computational efficiencies of the existing ones. In this survey of image restoration literature, different methods are categorized based on the noise domain these methods are entitled to access. The remainder of this chapter briefly delineate the main features in some of the most popular image restoration approaches.

2.2 Impulsive Noise Filters

Among the different types of noise models, impulse denoising has been one of the most well-studied problems. A quick browse on IEEE Xplore with a simple query “impulse filtering” returns more than 10,000 hits for papers published after year 2000. One gets slightly less than 8000 hits with a similar search on Science Direct. Broadly, these figures reveal the dynamic progress in impulse denoising, besides offering an impression on the knowledge wealth in this

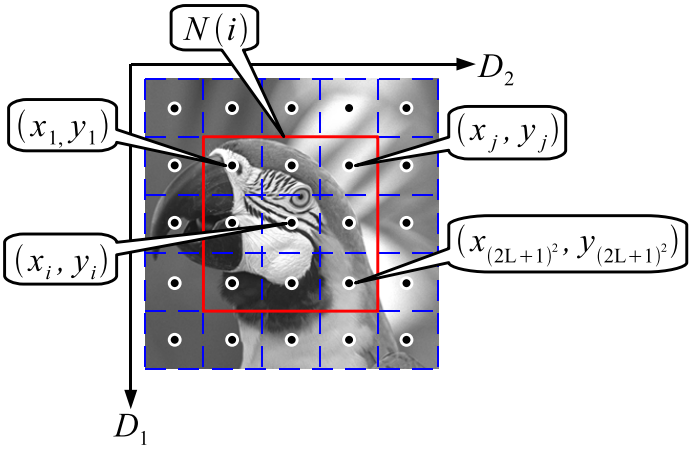

Figure 2.1: An illustration on the concept of search window $N(i)$ with the pixel of interest i centered around the neighboring pixels j. The pair of augmented variables (x,y) represents the pixel's spatial position x and photometric intensity y. The search window has a $(2L+1) \times (2L+1)$ odd dimension, whereas the image of size $M_1 \times M_2$ sits on a two-dimensional space defined by the axes D_1 and D_2.

area. However, these methods vary widely in their approaches. In [21], Yuksel provides an excellent overview of modern as well as classical impulse denoising techniques.

Before venturing forth, some notations to be used throughout the rest of this presentation are first defined. Here, a rectangular search window $N(i)$ is denoted as the $(2L+1) \times (2L+1)$ neighborhood centered at the pixel of interest i. Meanwhile, the neighboring pixels are denoted as j. Each pixel inside $N(i)$ carries a pair of pertinent values, namely, its spatial position x and its photometric intensity y. This concept is illustrated in Figure 2.1. As will be seen later in this chapter, most of the image restoration algorithms are designed to compute the value for pixel i by using some pixels j within a specified vicinity of $N(i)$. Below, some of the well-known impulse detectors and filters in literature are succinctly outlined based on their category.

2.2.1 Median Filter and Its Switching Variants

Specifically for the removal of impulse noise, nonlinear techniques can be considered as the state-of-the-art methods. Of them, the median filter [22, 23], which exploits the rank-order

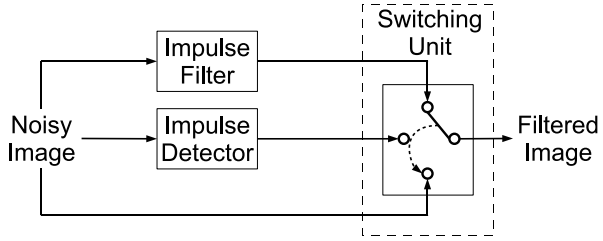

Figure 2.2: A general block diagram representation of switching scheme impulse filters (adapted from [26]).

information within the window $N(i)$, appears as a popular choice for suppressing impulse noise. The median filtering operation can be described by

$$\widetilde{y_i} = m_i = \text{median}\{y_j\}. \tag{2.1}$$

Gallagher *et al.* [24, 25] provide a theoretical analysis on the properties of median filter. By and large, median filtering is employed in a similar fashion as window-based filtering algorithms. It is applied in a raster-scan order and treats all pixels equally regardless of whether the pixels are corrupted or noise-free. Local information made up of image details and edges comprising of noise-free pixels are subjects to be filtered. Hence, ignoring such local information often renders desirable image details at best blurred and at worst missing upon filtering. Nonetheless, this drawback has been overcome with the inception of switching filters framework.

The pivotal role of switching filters is to discriminate noise pixels from the noise-free ones prior to applying nonlinear filtering. This role can be accomplished by incorporating the conventional median filtering framework with an impulse detector, which acts as a "switch." Figure 2.2 shows the general concept of switching filters. It is observed that switching filters that utilize such additional information can enjoy performance improvement over their nonswitching counterparts. In this survey, existing switching filters are classified into three categories: non-adaptive, adaptive, and iterative. Within each category, more advanced techniques are

integrated as part of the switching framework to obtain additional information about the image, e.g., local statistics and thresholds [27]. These sophisticated techniques include various order-statistics (e.g., median of absolute deviation (MAD) [28], pixel-wise MAD (PWMAD) [29], rank-order absolute difference (ROAD) [30], and rank-order logarithmic difference (ROLD) [31]), rank-order criterion [32, 33], variational-regularization [31, 34, 35], mathematical morphology [36, 37], threshold Boolean [38], logical representation [39, 40], and soft-computing [41, 42]. Technically, the high-complexity techniques are effective for switching filters because of their adaptive functionalities and advanced features to approximate nonstationary statistical characteristics of impulse noise.

The fundamental switching concept is first introduced by Sun and Neuvo [43] in 1994. As a modification to the median filter, the idea of impulse detector can be represented by

$$\alpha_i = \begin{cases} 1 & : \quad |y_i - m_i| > T_s, \\ 0 & : \quad |y_i - m_i| \leq T_s, \end{cases} \tag{2.2}$$

where T_s is a predefined threshold. In essence, $\alpha_i = 1$ indicates y_i is a corrupted pixel and the impulse filter is switched on. Otherwise, y_i is considered as noise-free and the impulse filter is switched off. The restoration term is then computed as

$$\widetilde{y_i} \quad = \quad \alpha_i m_i + (1 - \alpha_i) y_i. \tag{2.3}$$

Obviously, using the photometric distance measure $|y_i - m_i|$ in (2.2) cannot distinguish impulses present along thin lines. This is because thin lines are erred as impulsive pixels since the presence of thin lines is characterized by the significant difference between pixel intensities forming the thin lines with those of homogeneous neighborhood. In an immediate response, the impulse detector employing four Laplacian kernels K_p is used, each of which is sensitive to edges in a different orientation [44]. These Laplacian kernels are shown in Figure 2.3, while